IJMMM International Journal of Minerals, Metallurgy and Materials 矿物冶金与材料学报（英文版）

Influence of polymer solution on the morphology and local structure of NH_4ZnPO_4 powders synthesized by a simple precipitation method at room temperature

Santi Phumying, Thongsuk Sichumsaeng, Pinit Kidkhunthod, Narong Chanlek, Jessada Khajonrit, Somchai Sonsupap, and Santi Maensiri

Cite this article as:
Santi Phumying, Thongsuk Sichumsaeng, Pinit Kidkhunthod, Narong Chanlek, Jessada Khajonrit, Somchai Sonsupap, and Santi Maensiri, Influence of polymer solution on the morphology and local structure of NH_4ZnPO_4 powders synthesized by a simple precipitation method at room temperature, *Int. J. Miner. Metall. Mater.*, 29(2022), No. 2, pp. 298-304. https://doi.org/10.1007/s12613-020-2208-8

Articles you may be interested in

Gui-hua Liu, Zheng Li, Xiao-bin Li, Tian-gui Qi, Zhi-hong Peng, and Qiu-sheng Zhou, Precipitation of spherical boehmite from concentrated sodium aluminate solution by adding gibbsite as seed, *Int. J. Miner. Metall. Mater.*, 24(2017), No. 8, pp. 954-963. https://doi.org/10.1007/s12613-017-1483-5

Xiao-yi Shen, Hong-mei Shao, Ji-wen Ding, Yan Liu, Hui-min Gu, and Yu-chun Zhai, Zinc extraction from zinc oxidized ore using $(NH_4)_2SO_4$ roasting–leaching process, *Int. J. Miner. Metall. Mater.*, 27(2020), No. 11, pp. 1471-1481. https://doi.org/10.1007/s12613-020-2015-2

A. I. Noskov, A. Kh. Gilmutdinov, and R. M. Yanbaev, Effect of coaxial laser cladding parameters on bead formation, *Int. J. Miner. Metall. Mater.*, 24(2017), No. 5, pp. 550-556. https://doi.org/10.1007/s12613-017-1436-z

Mohammad Sefidmooy Azar, Shahram Raygan, and Saeed Sheibani, Effect of chemical activation process on adsorption of As(V) ion from aqueous solution by mechano-thermally synthesized zinc ferrite nanopowder, *Int. J. Miner. Metall. Mater.*, 27(2020), No. 4, pp. 526-537. https://doi.org/10.1007/s12613-019-1931-5

Betül Kafkaslıolu Yıldız, Hüseyin Yılmaz, and Yahya Kemal Tür, Influence of nickel addition on the microstructure and mechanical properties of Al_2O_3-5vol%ZrO_2 ceramic composites prepared via precipitation method, *Int. J. Miner. Metall. Mater.*, 26(2019), No. 7, pp. 908-914. https://doi.org/10.1007/s12613-019-1792-y

Lalinda Palliyaguru, Ushan S. Kulathunga, Lakruwani I. Jayarathna, Champa D. Jayaweera, and Pradeep M. Jayaweera, A simple and novel synthetic route to prepare anatase TiO_2 nanopowders from natural ilmenite via the H_3PO_4/NH_3 process, *Int. J. Miner. Metall. Mater.*, 27(2020), No. 6, pp. 846-855. https://doi.org/10.1007/s12613-020-2030-3

IJMMM WeChat

QQ author group

International Journal of Minerals, Metallurgy and Materials
Volume 29, Number 2, February 2022, Page 298
https://doi.org/10.1007/s12613-020-2208-8

Influence of polymer solution on the morphology and local structure of NH_4ZnPO_4 powders synthesized by a simple precipitation method at room temperature

Santi Phumying[1)], *Thongsuk Sichumsaeng*[1)], *Pinit Kidkhunthod*[2)], *Narong Chanlek*[2)], *Jessada Khajonrit*[1,3)], *Somchai Sonsupap*[1,3)], *and Santi Maensiri*[1,3),✉]

1) School of Physics, Institute of Science, Suranaree University of Technology, Nakhon Ratchasima 30000, Thailand
2) Synchrotron Light Research Institute (Public Organizer), Nakhon Ratchasima 30000, Thailand
3) SUT-NANOTEC RNN on Nanomaterials and Advanced Characterizations, Suranaree University of Technology, Nakhon Ratchasima 30000, Thailand
(Received: 4 August 2020; revised: 24 September 2020; accepted: 12 October 2020)

Abstract: NH_4ZnPO_4 powders were synthesized using a simple precipitation method at room temperature. The effects of polyvinyl pyrrolidone (PVP), polyvinyl alcohol (PVA), glucose, and hexadecyltrimethylammonium bromide (CTAB) solutions on the morphology and structure of the prepared samples were investigated. The phase composition and morphology of the prepared samples were characterized using X-ray diffraction and scanning electron microscopy, respectively. Depending on the polymer sources, the hexagonal structure prepared using non-surfactant of water completely changed to monoclinic structure when CTAB was added. X-ray absorption near-edge structure (XANES) and X-ray photoelectron spectroscopy (XPS) were performed to study the local structure and surface electronic structure of the prepared samples, confirming that the oxidation states of P and Zn ions are 5+ and 2+, respectively. On the basis of the results of inductively coupled plasma atomic emission spectroscopy (ICP-OES), the NH_4ZnPO_4 powders can be classified as a slow-release fertilizer where less than 15% of the ions were released in 24 h. A simple precipitation method using water, PVP, PVA, sucrose, and CTAB as a template can be used to synthesize NH_4ZnPO_4 powders. In addition, this method may be extended for the preparation of other oxide materials.

Keywords: ammonium zinc phosphate; precipitation method; morphology; X-ray absorption spectroscopy; ion release properties

1. Introduction

Chemical fertilizers are commonly used to provide nutrients in plants for optimal growth and production. However, the available plant production process is insufficient to support the rapid growth of food demand [1]. Hence, nano-fertilizers have been applied in plants to enhance crop yields by increasing seed germination, seedling growth rate, nitrogen metabolism, protein and carbohydrate synthesis, and durability. Nano-fertilizers can also be used in small quantity to increase the ease of use and reduce the economic cost compared with conventional fertilizers [2].

In recent years, slow-release ammonium metal phosphate ($NH_4M(II)PO_4H_2O$)-based fertilizers, where M is a metal atom, have been used [3]. Such fertilizers are environmental friendly because their negligible toxicity. Recently, many efforts have been devoted to improve the performance of these fertilizers by modifying their morphology, particle size, and doping [4]. Zinc is an essential micronutrient required for the normal growth and development of plants. This micronutrient promotes protein metabolism and reduces plant resistibility in unsuitable environments. For example, ammonium zinc phosphate (NH_4ZnPO_4) is as a good source of phosphorus, nitrogen, and zinc for plant production [5–6]. NH_4ZnPO_4 fertilizer can be synthesized hydrothermally under autogenous pressure at temperatures ranging from 100 to 250°C. It is also a good flame retardant in gas and condensed phases, and is safe while storing [7–8].

Until now, a method for the preparation of NH_4ZnPO_4 nanofertilizer is lacking. Hence, a suitable method to prepare nano-NH_4ZnPO_4 is important to improve crop yield. Recent studies have synthesized nanostructures by using various techniques, such as sol–gel, hydrothermal, and co-precipitation methods. The changes in size and morphology can be determined through the intermolecular interactions of atoms in the compound, such as solvent type, compound permanence, material type, and supersaturation degree [9–10]. The co-precipitation method is commonly used to prepare nanomaterials; in this method, the size and shape can be controlled by varying the amount and type of solvent. For example, $NH_4CoPO_4{\cdot}H_2O$ nano–micro-particles with sizes ranging from 200 to 4000 nm can be achieved by using a simple

✉ Corresponding author: Santi Maensiri E-mail: santimaensiri@g.sut.ac.th, santimaensiri@gmail.com

co-precipitation method in ethylene glycol solvent [9].

In this work, we report the synthesis of ammonium zinc phosphate fertilizer by using a simple precipitation method at room temperature with various solution templates, including polyvinyl pyrrolidone (PVP), polyvinyl alcohol (PVA), glucose, and hexadecyltrimethylammonium bromide (CTAB). The structure, morphology, local structure, and surface electronic structure properties of the NH_4ZnPO_4 products synthesized with different precursors were characterized using X-ray diffraction (XRD), field emission scanning electron microscopy (FE-SEM), inductively coupled plasma atomic emission spectroscopy (ICP-OES), X-ray photoelectron spectrometry (XPS), and X-ray absorption spectroscopy (XAS).

2. Experimental

2.1. Material preparation

The samples were prepared using a simple precipitation method consisting of starting chemicals of zinc(II) chloride ($ZnCl_2$) used as the metal sources and polymer solutions. In this work, 5% by weight of the polymer was mixed with 100 mL of deionized water under vigorous stirring at 27°C until a homogeneous solution was obtained. Water, PVP, PVA, glucose, and CTAB were used as the polymer sources. The metal sources (20 mmol) and phosphoric acid solution (H_3PO_4, 70wt%, 3 mL) were dissolved in deionized water and polymer solution (50 mL) to form a clear solution. The mixed solution was precipitated by adding ammonium solution (25wt%) with vigorous stirring until pH = 7. The precipitates were washed several times with deionized water and ethanol. Then, the samples were dried at 70°C in air. A schematic of the preparation of the samples is shown in Fig. 1. Finally, the samples were stored in a desiccator for further characterization.

2.2. Materials characterization

The prepared products were characterized using XRD, SEM, XPS, and XAS. The XRD patterns were examined on a Bruker D8 Advance (USA) with Cu K_α radiation (λ = 0.154184 nm) to confirm the phase information of the samples. Scanning electron microscopy and energy dispersive spectrometry were performed using Zeiss AURIGA FIB-SEM (Germany) with FE-SEM at 7 kV to reveal the morphology of the prepared samples. Transmission electron microscopy was performed with a FEI Tecnai G2 F20 field emission transmission electron microscope (USA) operated at 200 kV. X-ray absorption near-edge structure (XANES) spectra at Zn K-edge were collected at the SUT–NANOTEC–SLRI XAS beamline (BL 5.2) at the Synchrotron Light Research Institute of Thailand to obtain the oxidation states of the samples. The XANES spectra were obtained in transmission mode using Ge (220) double crystal monochromators with an energy resolution of 2×10^{-4} eV.

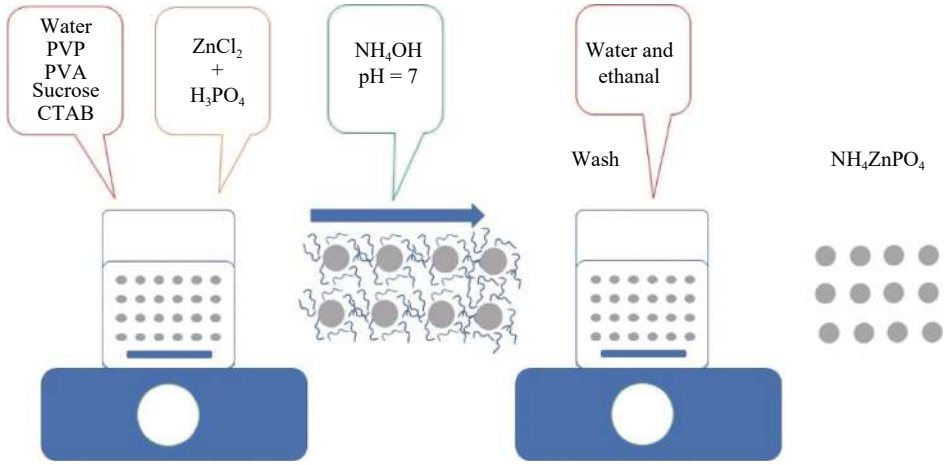

Fig. 1. Schematic of the formation of NH_4ZnPO_4 powder synthesized by a chemical precipitation method using water, PVP, PVA, sucrose, and CTAB solutions.

2.3. Ion release properties

In addition to crystal size and morphology, ion release is an important property that determines the potential use of materials as fast- or slow-release fertilizers. In this study, the NH_4ZnPO_4 samples prepared using water, PVP, PVA, sucrose, and CTAB solutions were chosen to study the ion release. In this experiment, the aqueous ion release at room temperature was examined in the prepared solution (0.5 g of the dried sample dissolved in 50 mL of deionized water), which was stirred continuously for 24 h. The sample was collected by filtering with a 0.22 μm filter membrane and subjecting to high-speed centrifugation at 8000 r/min. Finally, the Zn^{2+} and P^{5+} concentrations in the supernatant were determined using ICP-OES (Optima 2100 DV ICP-OES, Perkin Elmer Instruments, USA).

3. Results and discussion

3.1. Structural and morphological characterization

Fig. 2 shows the XRD patterns of the prepared samples. The XRD patterns of the prepared NH_4ZnPO_4 samples show the formation of a hexagonal structure within space group

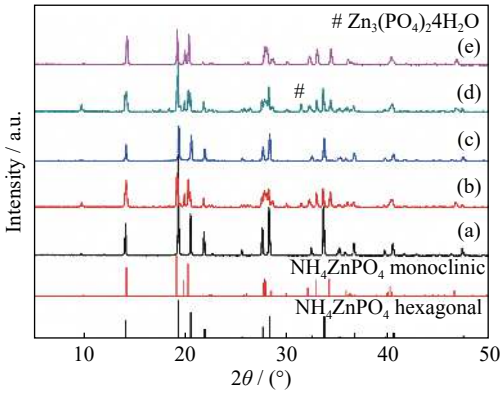

Fig. 2. XRD patterns of the NH_4ZnPO_4 powder prepared by using (a) water, (b) PVP, (c) PVA, (d) sucrose, and (e) CTAB.

P63 [11]. The diffraction peaks of the NH_4ZnPO_4 sample mainly consist of (100), (101), (200), (002), (201), (210), (211), (202), (103), (220), (222), and (123) planes, which agree with the standard data (JCPDS NO.89-6315). In addition, the PVP and sucrose conditions present the phase impurities of NH_4ZnPO_4 with monoclinic structure and $Zn_3(PO_4)_2 4H_2O$. The CTAB condition shows only NH_4ZnPO_4 monoclinic structure, which is in good agreement with the standard data (JCPDS NO.88-1126) and is consistent with the literatures [12–13].

The unit cell parameters (*a*, *b*, and *c*), cell volume (*V*), expected profile residual (R_{exp}), profile residual (R_p), weighted profile residual (R_{wp}), and goodness-of-fit (GOF) values of all NH_4ZnPO_4 samples were calculated using Rietveld refinement unit cell analysis (TOPAS software), and the results are summarized in Table 1. Using the medium solution of PVP, sucrose, and CTAB can change the phase structure from hexagonal to NH_4ZnPO_4 monoclinic. Moreover, the CTAB condition showed an XRD pattern of only NH_4ZnPO_4 monoclinic structure. The growth process of NH_4ZnPO_4 by adding CTAB is different. The surfactant reduces the surface tension of the solution and then lowers the energy needed to form a new phase of NH_4ZnPO_4 monoclinic structure at a low supersaturation [12]. In another case, CTAB could also be considered to influence the disintegration of zinc and the growth of NH_4ZnPO_4 through electrostatic and stereochemical effects [14]. The hexagonal and monoclinic structures of NH_4ZnPO_4 can be used as fertilizers [15].

Table 1. Lattice parameters (*a*, *b*, c, and *β* angle), cell volume (*V*), Rietveld refinement parameters (R_p, R_{exp}, R_{wp}, and GOF), phase composition, and ion releases of the NH_4ZnPO_4 powder prepared using different media (water, PVP, PVA, sucrose, and CTAB)

Media	*a* / nm	*b* / nm	*c* / nm	*β* / (°)	*V* / (10^6 pm^3)	Space group	R_p / %	R_{exp} / %
Water	1.0692	1.0692	0.8709	90	862.13	P63	4.67	2.46
PVP	1.0691	1.0691	0.8707	90	861.96	P63	3.84	2.27
PVA	1.0693	1.0693	0.8708	90	862.40	P63	3.77	2.77
Sucrose	1.0690	1.0690	0.8706	90	861.76	P63	4.39	2.28
CTAB	0.8790	0.5450	0.8960	90.34	429.16	P21	3.03	2.56

Media	R_{wp} / %	GOF / %	Phase composition / %			Zn release / (mg·L^{-1})	P release / (mg·L^{-1})
			Hexagonal	Monoclinic	Hopeite		
Water	6.66	2.70	100	0	0	0.34 ± 0.01	33.57 ± 3.15
PVP	5.94	2.62	13.88	69.86	16.26	1.65 ± 0.02	41.97 ± 5.90
PVA	5.03	1.82	100	0	0	0.66 ± 0.01	34.02 ± 4.10
Sucrose	6.02	2.64	20.44	56.30	23.26	4.21 ± 0.02	48.29 ± 3.17
CTAB	3.88	1.51	0	100	0	0	26.57 ± 3.32

Fig. 3 shows the FE-SEM images of the NH_4ZnPO_4 powders prepared using water and polymer sources of PVP, PVA, sucrose, and CTAB solutions. As shown in Fig. 3, the microparticles are about 0.4–10 μm in size. The results confirm that the ammonium zinc phosphate provides different morphologies and sizes. During precipitation, morphological properties such as particle size depend not only on the chemical reaction of the compound but also on the other experimental conditions, such as surfactants and solvents. Herein, NH_4ZnPO_4 powders were synthesized in water solution as a reference, and results showed that the product has normal morphology. As shown in Fig. 3(a), the microrods obtained using non-surfactant of water formed through self-assembly [11]. The ion concentration profiles in water are defined by the speciation diagrams of phosphoric acid (H_3PO_4) and ammonia solution. The chemical reaction of ammonium zinc phosphate can be expressed by the following equation:

$$ZnCl_2 + NH_4OH + H_3PO_4 \rightarrow NH_4ZnPO_4 + H_2O + 2HCl$$

In comparison, the use of surfactant as a template provides various morphologies of NH_4ZnPO_4. The morphologies of the prepared NH_4ZnPO_4 particles are controlled by the relative growth rate of different crystal facets [16]. Moreover, the rare earth orthophosphate with hexagonal phase shows a high anisotropic structure, which strongly influences their morphological evolution [12]. The phosphates with monoclinic structure have less anisotropy and low tendency to grow along a random direction [17]. Thus, the use of PVP, PVA, sucrose, and CTAB solutions can change the morphology of NH_4ZnPO_4 to the nanoparticle size.

The possible formation mechanisms of NH_4ZnPO_4 microstructures by using water and polymer sources of PVP, PVA, sucrose and CTAB are proposed in Fig. 4. In general, the formation of particles is related to nucleation and crystal growth [18–19]. Nucleation consists of the formation of

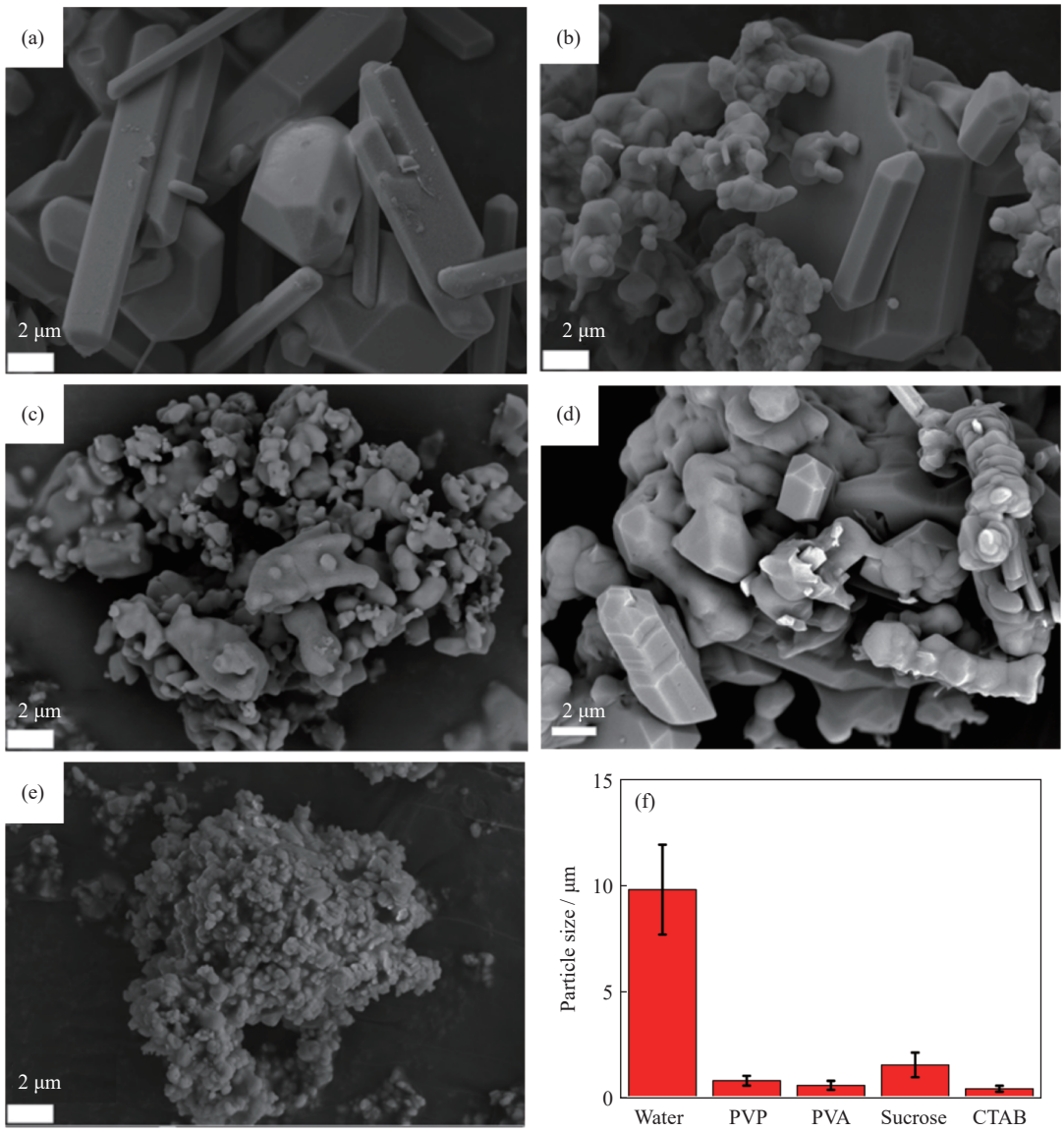

Fig. 3. SEM images of the NH_4ZnPO_4 powders prepared using a chemical precipitation method with (a) water, (b) PVP, (c) PVA, (d) sucrose, and (e) CTAB; (f) corresponding average particle sizes of NH_4ZnPO_4 powders.

stable nuclei and the growth of critical nuclei, resulting in the generation of large crystals in crystal growth [20–22]. In the absence of a surfactant as shown in Fig. 4, the secondary particles resulting from the aggregation of the primary particles self-assemble into the microrods. Particle growth is related to the adsorption of surfactants onto particular crystallographic facets of the growing crystal [23]. The addition of surfactants such as PVP, PVA, sucrose, and CTAB into the nucleation process can affect the surface energy, and thus control the nucleation rate [24]. Slower nucleation rate corresponds to larger particle size. The particles agglomerated with a microrod-like shape when the nonionic surfactant of PVP was added. These results may be attributed to the low PVP concentration. The explanations are as follows [23]: (i) the adsorption of PVP was insufficient for the effective coverage of the NH_4ZnPO_4 phase, resulting in particle agglomeration; (ii) the particles underwent continuous self-assembly, resulting in a microrod-like shape. For PVA, a polymer chain of PVA adsorbed onto the particle surface through non-cova-

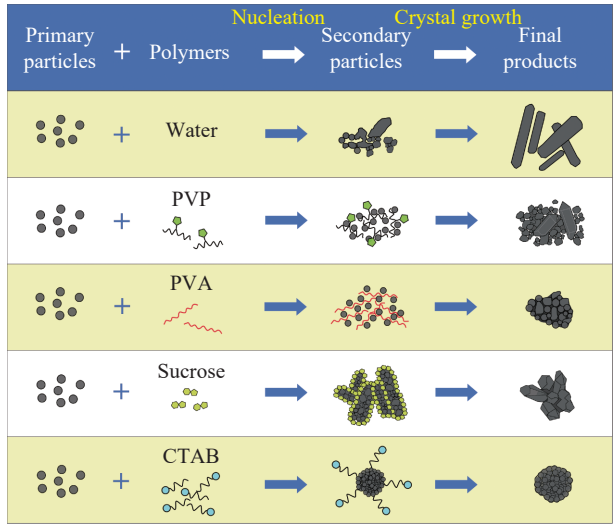

Fig. 4. Possible formation mechanisms of NH_4ZnPO_4 microstuctures prepared by using water and polymer sources of PVP, PVA, sucrose, and CTAB.

lent bonding of hydroxyl groups. The adsorbed PVA formed a multilayer coating around the particles as a water-protective agent, decreasing the particle size and preventing agglomeration [25]. In the case of sucrose, the multiple hydroxyl groups of a large molecular size of non-reducing sucrose adsorbed onto certain crystal planes as a coating agent to form steric hindrance. Thus, sucrose may possibly be transformed to glucose and gluconic acid that were coated on the particle surface, decreasing the particle size [26–27]. The hydrophobic tail of CTAB is adsorbed onto the particle surface, and the adsorbed CTAB hinders other nutrients to attach to the surface [28]. Then, the growth rate slows down, resulting in the agglomeration of particles forming as bulk products of sphere [29].

3.2. Iron release properties

The ion release measurement was used to clarify the type of fertilizer of all NH_4ZnPO_4 samples prepared using water, PVP, PVA, sucrose, and CTAB solutions. The ion release properties are summarized in Table 1. The P ion releases of (33.57 ± 3.15), (41.97 ± 5.90), (34.02 ± 4.10), (48.29 ± 3.17), and (26.57 ± 3.32) $mg·L^{-1}$ were observed in the NH_4ZnPO_4 prepared in water, PVP, PVA, sucrose, and CTAB solutions, respectively. The Zn ion releases of (0.34 ± 0.01), (1.65 ± 0.02), (0.66 ± 0.01), (4.21 ± 0.02), and 0 $mg·L^{-1}$ were observed in the NH_4ZnPO_4 prepared in water, PVP, PVA, sucrose, and CTAB solutions, respectively. These results indicate that more Zn and P ions with hexagonal structure were released than those with monoclinic structure. In addition, Zn and P ions were released with a higher proportion of Hopeite. Considering the molar mass ratio of NH_4ZnPO_4 prepared in sucrose solution, the mass of P and Zn ions was calculated to be around 540 mg in 1 g of this compound. After combining the value of P and Zn ion release (52.5 $mg·L^{-1}$), approximately 5 mg out of 540 mg of P and Zn ions corresponding to around 1% of the total mass was released in 24 h. On the basis of the obtained results, our NH_4ZnPO_4 powders can be classified as slow-release fertilizers where less than 15% of the ions were released in 24 h [30]. In specific, the Zn ion release of 4.17 $mg·L^{-1}$ is comparable with previous reports on $Zn(OH)_2$ (9.62 $mg·L^{-1}$) [31], the core–shell $ZnSO_4$ (3.8 $mg·L^{-1}$) [32], the zeolite-based $ZnSO_4$ (4.5 $mg·L^{-1}$) [33], and the commercial ZnO-based fertilizer (1–2 $mg·L^{-1}$) [31]. These results suggest that our simple facile route can be used to synthesize a NH_4ZnPO_4-based slow-release fertilizer.

3.3. X-ray absorption study

The XANES spectra of NH_4ZnPO_4 of Zn K-edge XANES were obtained at the energy range of 9600–9760 eV to examine the oxidation states of the iron element in the samples. Fig. 5 shows the normalized Zn K-edge XANES spectra of the NH_4ZnPO_4 H_2O prepared using water, PVP, PVA, sucrose, and CTAB solutions, in comparison with the standard compounds of Zn^{0+} and Zn^{2+}. The edge energy positions of the NH_4ZnPO_4 H_2O samples were 9662.60, 9662.62, 9662.27, 9662.54, and 9662.50 eV, which lied on the edge

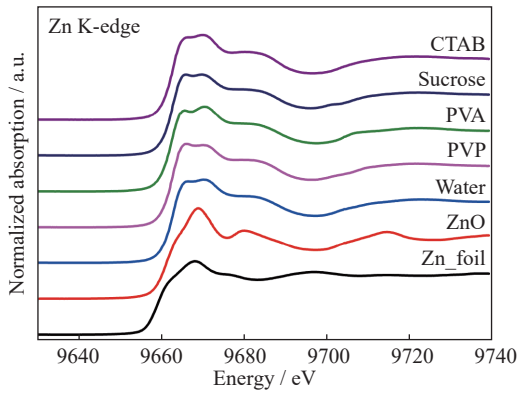

Fig. 5. Zn K-edge XANES spectra of NH_4ZnPO_4 powder prepared by chemical precipitation.

energy positions of ZnO (E_0 = 9662.69 eV) standard sample. These results imply that the oxidation state of Zn ions in all the prepared samples is 2+.

Fig. 6 shows the normalized P K-edge XANES spectra of the NH_4ZnPO_4 prepared with water, PVP, PVA, sucrose, and CTAB conditions, in comparison with the standard compounds of P^{0+} and P^{5+}. The results indicate that the spectra of all samples show similar features. The edge energy positions of the samples match with that of the KH_2PO_4 standard sample. These results suggest that the oxidation state of P ions in all the prepared samples is 5+.

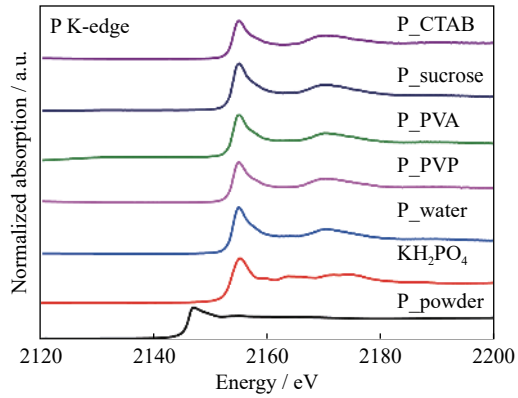

Fig. 6. P K-edge XANES spectra of NH_4ZnPO_4 powder prepared by chemical precipitation.

3.4. X-ray photoelectron spectroscopy

The chemical compositions of all the prepared samples were examined by XPS. The XPS spectra of ammonium zinc phosphate are shown in Fig. 7, and these spectra were calibrated using C 1s (284.8 eV) as the reference. The XPS spectra of the Zn 2p region of NH_4ZnPO_4 show Zn^{2+} at binding energy (BE) of ~1022 eV ($2p_{3/2}$), indicating that all samples have Zn^{2+} in the structure. The XPS spectra of the P 2p region of the NH_4ZnPO_4 samples prepared using water, PVP, PVA, sucrose, and CTAB solutions are shown in Fig. 8. All of the NH_4ZnPO_4 samples exhibited the only peak of P 2p at BE of ~134 eV ($2p_{3/2}$). The XPS results for other phosphates also showed that the products were completely formed in the stoichiometric ratio and that P existed in the P^{5+} state. These

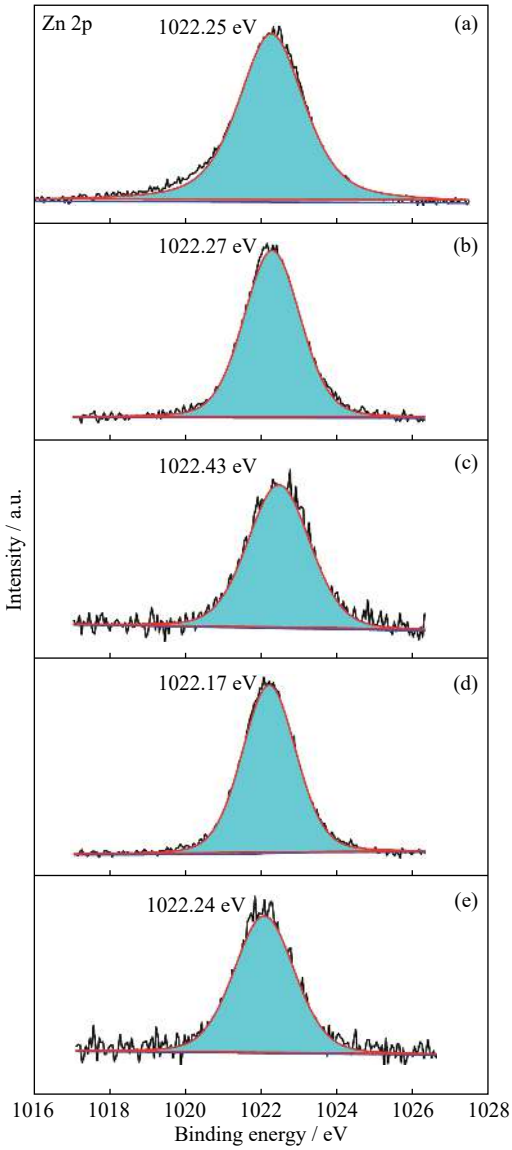

Fig. 7. Curve-fitting for Zn 2p and XPS spectra of NH_4ZnPO_4 samples prepared with (a) water, (b) PVP, (c) PVA, (d) sucrose, and (e) CTAB.

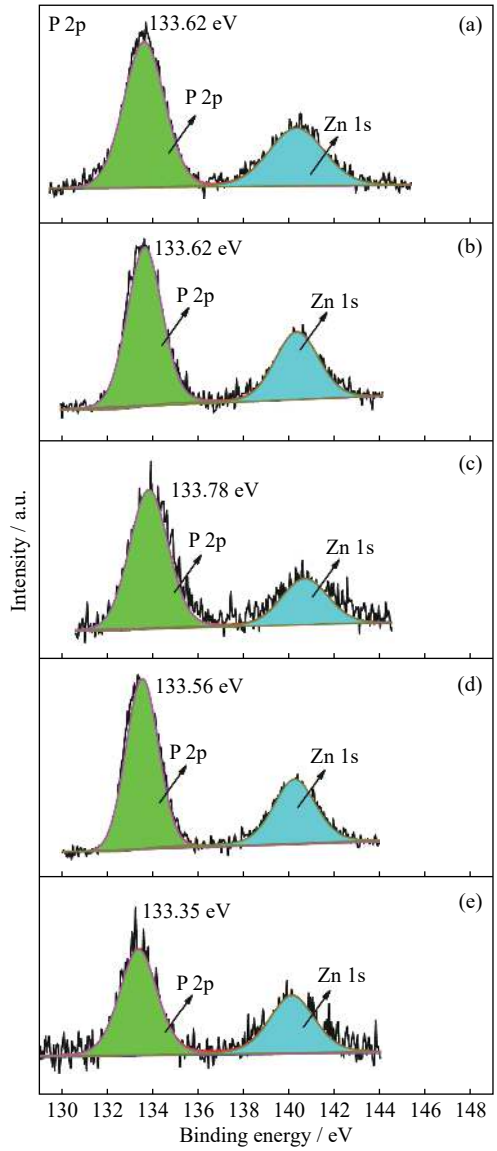

Fig. 8. Curve-fitting for P 2p and XPS spectra of NH_4ZnPO_4 samples prepared with (a) water, (b) PVP, (c) PVA, (d) sucrose, and (e) CTAB.

results indicate that the presence of P^{5+} (NH_4ZnPO_4) in the sample corresponds to the XRD and XAS results.

4. Conclusion

NH_4ZnPO_4 powders with particle sizes of ~0.1–10 μm used as slow-release fertilizers were successfully prepared using a simple and polymers-assisted co-precipitation method. The use of PVP, PVA, sucrose, and CTAB solutions affects the morphology of the prepared samples. Depending on the type of polymer used, XRD results indicate that the hexagonal structure changes to monoclinic structure in the absence of polymer solution when CTAB is added. XANES and XPS results confirm that the oxidation states of Zn and P ions in all the prepared samples are 2+ and 5+, respectively. The simple co-precipitation method using only water solution can also produce NH_4ZnPO_4 particles. This simple method can be extended to prepare other metal-oxide or complex-oxide micro–nano-particles. In addition, the resulting NH_4ZnPO_4 shows great potential applications in slow-release fertilizers to reduce the amount of chemicals used in plants.

Acknowledgements

The authors would like to thank the Synchrotron Light Research Institute (Public Organization), Nakhon Ratchasima, Thailand for XPS and XANES facilities. This work was supported by Suranaree University of Technology (SUT)-PhD Fund from Suranaree University of Technology. This work was also supported by the SUT and by the Office of the Higher Education Commission under NRU Project of Thailand, Suranaree University of Technology, Nakhon Ratchasima, Thailand.

Conflict of Interest

The authors declare no conflict of interest.

References

[1] X. Zhang, E.A. Davidson, D.L. Mauzerall, T.D. Searchinger, P. Dumas, and Y. Shen, Managing nitrogen for sustainable development, *Nature*, 528(2015), No. 7580, p. 51.

[2] F. Zulfiqar, M. Navarro, M. Ashraf, N.A. Akram, and S. Munné-Bosch, Nanofertilizer use for sustainable agriculture: Advantages and limitations, *Plant Sci.*, 289(2019), art. No. 110270.

[3] H. Pang, Z.Z. Yan, W.Q. Wang, Y.Y. Wei, X.X. Li, J. Li, J. Chen, J.S. Zhang, and H.H. Zheng, Template-free controlled fabrication of $NH_4MnPO_4{\cdot}H_2O$ and $Mn_2P_2O_7$ micro-nanostructures and study of their electrochemical properties, *Int. J. Electrochem. Sci.*, 7(2012), No. 12, p. 12340.

[4] X.G. Wang, S.Y. Lü, C.M. Gao, X.B. Xu, Y. Wei, X. Bai, C. Feng, N.N. Gao, M.Z. Liu, and L. Wu, Biomass-based multifunctional fertilizer system featuring controlled-release nutrient, water-retention and amelioration of soil, *RSC Adv.*, 4(2014), No. 35, p. 18382.

[5] G.L. Bridger, M.L. Salutsky, and R.W. Starostka, Micronutrient sources, metal ammonium phosphates as fertilizers, *J. Agric. Food Chem.*, 10(1962), No. 3, p. 181.

[6] M. Kalbasi, G.J. Racz, and L.A. Lewen-Rudgers, Reaction products and solubility of applied zinc compounds in some Manitoba soils, *Soil Sci.*, 125(1978), No. 1, p. 55.

[7] L.M. Lapina, Metal ammonium phosphates and their new applications, *Russ. Chem. Rev.*, 37(1968), No. 9, p. 693.

[8] A.Q. Yuan, J. Wu, L.J. Bai, S.M. Ma, Z.Y. Huang, and Z.F. Tong, Standard molar enthalpies of formation for ammonium/3d-transition metal phosphates $NH_4MPO_4{\cdot}H_2O$ (M = Mn^{2+}, Co^{2+}, Ni^{2+}, Cu^{2+}), *J. Chem. Eng. Data*, 53(2008), No. 5, p. 1066.

[9] H. Pang, Z.Z. Yan, W.Q. Wang, J. Chen, J.S. Zhang, and H.H. Zheng, Facile fabrication of $NH_4CoPO_4{\cdot}H_2O$ nano/microstructures and their primarily application as electrochemical supercapacitor, *Nanoscale*, 4(2012), No. 19, p. 5946.

[10] K. Byrappa, C.K. Chandrashekar, B. Basavalingu, K.M. LokanathaRai, S. Ananda, and M. Yoshimura, Growth, morphology and mechanism of rare earth vanadate crystals under mild hydrothermal conditions, *J. Cryst. Growth*, 306(2007), No. 1, p. 94.

[11] W.T.A. Harrison, A.N. Sobolev, and M.L.F. Phillips, Hexagonal ammonium zinc phosphate, $(NH_4)ZnPO_4$, at 10 K, *Acta Crystallogr. Sect. C: Cryst. Struct. Commun.*, 57(2001), No. 5, p. 508.

[12] B. Yan and J.F. Gu, Morphology controlled solvo-thermal synthesis and luminescence of NH_4ZnPO_4: Eu^{3+} submicrometer phosphor, *J. Alloys Compd.*, 479(2009), No. 1-2, p. 536.

[13] D. Yue, W. Lu, L. Jin, C.Y. Li, W. Luo, M.N. Wang, Z.L. Wang, and J.H. Hao, Controlled synthesis, asymmetrical transport behavior and luminescence properties of lanthanide doped ZnO mushroom-like 3D hierarchical structures, *Nanoscale*, 6(2014), No. 22, p. 13795.

[14] X.M. Sun, X. Chen, Z.X. Deng, and Y.D. Li, A CTAB-assisted hydrothermal orientation growth of ZnO nanorods, *Mater. Chem. Phys.*, 78(2003), No. 1, p. 99.

[15] G.W. Rehm, R.A. Wiese, and G.W. Hergert, Response of corn to zinc source and rate of zinc band applied with either orthophosphate or polyphosphate, *Soil Sci.*, 129(1980), No. 1, p. 36.

[16] Y. Li, Q.Y. Liu, and W.J. Shen, Morphology-dependent nanocatalysis: Metal particles, *Dalton Trans.*, 40(2011), No. 22, p. 5811.

[17] Z. Amghouz, B. Ramajo, S.A. Khainakov, I. da Silva, G.R. Castro, J.R. García, and S. García-Granda, Dimensionality changes in the solid phase at room temperature: 2D → 1D → 3D evolution induced by ammonia sorption–desorption on zinc phosphates, *Chem. Commun.*, 50(2014), No. 51, p. 6729.

[18] N.T.K. Thanh, N. Maclean, and S. Mahiddine, Mechanisms of nucleation and growth of nanoparticles in solution, *Chem. Rev.*, 114(2014), No. 15, p. 7610.

[19] Q. Chen, Y.Q. Wang, M.Y. Zheng, H. Fang, and X. Meng, Nanostructures confined self-assembled in biomimetic nanochannels for enhancing the sensitivity of biological molecules response, *J. Mater. Sci.: Mater. Electron.*, 29(2018), No. 23, p. 19757.

[20] D.D. Patel and B.D. Anderson, Maintenance of supersaturation II: Indomethacin crystal growth kinetics versus degree of supersaturation, *J. Pharm. Sci.*, 102(2013), No. 5, p. 1544.

[21] T.T. Jiang, Y.Q. Wang, D.W. Meng, X.L. Wu, J.X. Wang, and J.Y. Chen, Controllable fabrication of CuO nanostructure by hydrothermal method and its properties, *Appl. Surf. Sci.*, 311(2014), p. 602.

[22] Y.Q. Wang, T.T. Jiang, D.W. Meng, J. Yang, Y.C. Li, Q. Ma, and J. Han, Fabrication of nanostructured CuO films by electrodeposition and their photocatalytic properties, *Appl. Surf. Sci.*, 317(2014), p. 414.

[23] M.Y. Zhu, Y. Wang, D.H. Meng, X.Z. Qin, and G.W. Diao, Hydrothermal synthesis of hematite nanoparticles and their electrochemical properties, *J. Phys. Chem. C*, 116(2012), No. 30, p. 16276.

[24] Z.F. Jiang, J.M. Xie, D.L. Jiang, X.J. Wei, and M. Chen, Modifiers-assisted formation of nickel nanoparticles and their catalytic application to p-nitrophenol reduction, *CrystEngComm*, 15(2013), No. 3, p. 560.

[25] A. Kyrychenko, D.A. Pasko, and O.N. Kalugin, Poly(vinyl alcohol) as a water protecting agent for silver nanoparticles: The role of polymer size and structure, *Phys. Chem. Chem. Phys.*, 19(2017), No. 13, p. 8742.

[26] X.H. Sun, C.M. Zheng, F.X. Zhang, Y.L. Yang, G.J. Wu, A.M. Yu, and N.J. Guan, Size-controlled synthesis of magnetite (Fe_3O_4) nanoparticles coated with glucose and gluconic acid from a single Fe(III) precursor by a sucrose bifunctional hydrothermal method, *J. Phys. Chem. C*, 113(2009), No. 36, p. 16002.

[27] N. Treesukkasem, C. Chokradjaroen, S. Theeramunkong, N. Saito, and A. Watthanaphanit, Synthesis of Au nanoparticles in natural matrices by liquid-phase plasma: Effects on cytotoxic activity against normal and cancer cell lines, *ACS Appl. Nano Mater.*, 2(2019), No. 12, p. 8051.

[28] Y.C. Pan, D. Heryadi, F. Zhou, L. Zhao, G. Lestari, H.B. Su, and Z.P. Lai, Tuning the crystal morphology and size of zeolitic imidazolate framework-8 in aqueous solution by surfactants, *CrystEngComm*, 13(2011), No. 23, p. 6937.

[29] T. Asgari-Vadeghani, D. Ghanbari, M.R. Mozdianfar, M. Salavati-Niasari, S. Bagheri, and K. Saberyan, Sugar and surfactant-assisted synthesis of $Mg(OH)_2$ nano-flower and PVA nanocomposites, *J. Clust. Sci.*, 27(2016), No. 1, p. 299.

[30] M.E. Trenkel, *Slow- and Controlled-release and Stabilized Fertilizers: An Option for Enhancing Nutrient Use Efficiency in Agriculture*, International fertilizer industry Association, Paris, 2010, p. 14.

[31] P. Li, Z.P. Xu, M.A. Hampton, D.T. Vu, L.B. Huang, V. Rudolph, and A.V. Nguyen, Control preparation of zinc hydroxide nitrate nanocrystals and examination of the chemical and structural stability, *J. Phys. Chem. C*, 116(2012), No. 18, p. 10325.

[32] M. Yuvaraj and K.S. Subramanian, Controlled-release fertilizer of zinc encapsulated by a manganese hollow core shell, *Soil Sci. Plant Nutr.*, 61(2015), No. 2, p. 319.

[33] M. Yuvaraj and K.S. Subramanian, Development of slow release Zn fertilizer using nano-zeolite as carrier, *J. Plant Nutr.*, 41(2018), No. 3, p. 311.